ORIGINAL RESEARCH

Experimental myositis: an optimised version of C-protein-induced myositis

Margherita Giannini ![ORCID] ,[1,2] Daniela Rovito,[3] Mustapha Oulad-Abdelghani,[3] Nadia Messaddeq,[3] Léa Debrut,[2] Giulia Quiring,[2] Pascal Kessler,[4] Anne-Laure Charles,[2] Bernard Geny,[2,5] Daniel Metzger,[3] Gilles Laverny,[3] Alain Meyer ![ORCID] [1,2,6]

Correspondence to
Dr Margherita Giannini; gianninim@unistra.fr

ABSTRACT

Introduction Inflammatory myopathies (IM) are a group of severe autoimmune diseases, sharing some similarities, whose cause is unknown and treatment is empirical. While C-protein-induced myositis (CIM), the most currently used mouse model of IM, has removed some roadblocks to understand and improve the treatment of IM, it has only been partially characterised and its generation limited by poor reproducibility. This study aimed at optimising the generation and the characterisation of CIM.

Methods In silico analysis was run to identify the top three specific and immunogenic regions of C-protein. The cognate polypeptides were synthesised and used to immunise C57BL/6N mice. Grip strength, walking ability, serum creatine kinase levels and muscle pathology (histological and electron microscopic features) were assessed. Immune cell proportions and interferon signature in muscles were also determined.

Results Among the three C-protein polypeptides with the highest immunogenic score, immunisation with the amino acids 965–991 induced the most severe phenotype (experimental myositis (EM)) characterised by 37% decrease in strength, 36% increase in hind base width, 45% increase in serum creatine-kinase level and 80% increase in histological inflammatory score. Optical and electron microscopy revealed mononuclear cell infiltrate, myofibre necrosis, atrophy, major histocompatibility complex-I expression as well as sarcolemmal, sarcomeric and mitochondrial abnormalities. Autoantibodies targeting C-protein, proinflammatory T-lymphocytes, macrophages, and type I and II interferon-stimulated transcripts were detected within the muscle of EM mice.

Conclusion EM recapitulates the common hallmarks of IM. This costless, high throughput, reproducible and robust model, generated in the most commonly used background for genetically engineered mice, may foster preclinical research in IM.

WHAT IS ALREADY KNOWN ON THIS TOPIC

⇒ C-protein-induced myositis is currently the most used model of inflammatory myopathies (IM), but has been partially characterised and its generation is limited by reproducibility issues.

WHAT THIS STUDY ADDS

⇒ Immunisation against the polypeptide encompassing C-protein amino acids 965–991 induces a costless, high-throughput, reproducible and robust model of myositis (experimental myositis) that recapitulates the common hallmarks of IM.

HOW THIS STUDY MIGHT AFFECT RESEARCH, PRACTICE OR POLICY

⇒ Experimental myositis, generated in the most used background for genetically engineered mice (C57BL/6N), might foster preclinical research in IM.

INTRODUCTION

Inflammatory myopathies (IM) are rare autoimmune diseases, with a female-to-male ratio of 2.4/1,[1] which include dermatomyositis, immune-mediated necrotising myopathy, inclusion body myositis, anti-synthetase syndrome and scleromyositis.[2–4] Despite their differences, these subgroups share common characteristics[5 6] including proximal weakness, increased serum creatine kinase (CK) levels and histopathological lesions of the skeletal muscle (ie, mononuclear cell infiltrates and myofibre abnormalities). Although the severity and the extent of the myofibre lesions vary among subgroups, some (ie, major histocompatibility complex (MHC)-I expression, atrophy, necrosis, mitochondrial abnormalities, sarcolemmal irregularities and sarcomeric disruptions) are common to all IM subtypes.[7–9] Similarly, although their proportions vary among subgroups, T lymphocyte and macrophage infiltrate[7] along with interferon (IFN)-I (ie, *ISG15, IFIT3, IFI44, RSAD2*)[10–13] and IFN-II (ie, *GBP1, GBP2, PSMB8, CXCL9*)[12–15] signature within the muscle are found in all IM subtypes.[16] In addition, it has been recently shown that myositis-specific autoantibodies infiltrate muscle fibres and disrupt the function of their target autoantigens, playing a crucial role in IM pathogenesis.[17] These findings

further indicate that common pathophysiological pathways underpin these diseases.[6]

IM is associated with a decreased quality of life and increased mortality.[18 19] The aetiology of IM is unknown. Current treatments are empirical,[20] partially effective and prone to many side effects. Several mouse models of IM have been established to foster a better understanding of their pathophysiology and to test new candidate drugs.[21] Although these models recapitulate some aspects of the disease and have been successfully used to explore preclinical drug efficacy, they have only been partially characterised, and their generation is limited by financial and technical issues.

The most widely used model of IM is C-protein-induced myositis (CIM),[22–26] which is based on a single intradermal injection of a recombinant polypeptide encompassing amino acids (aa) 284–580 of the human fast-type myosin-binding-protein C (MYBPC, hereafter termed C-protein). CIM mice present a decrease in running ability, serum autoantibodies targeting C-protein, as well as T cell and macrophage infiltrates within the muscle. CD8+T cells cytotoxicity is responsible for muscle injury in CIM.[27 28] Muscle inflammation peaks at day (D) 21 after immunisation and begins to resolve after D28.[23] However, muscle fibre abnormalities, the detailed composition of the inflammatory infiltrate as well as IFN signature in CIM mice have not been reported.

The CIM model is also limited by both reproducibility and cost. Native C-protein is expensive: several mice are required to extract a protein that only accounts for approximately 2% of the entire amount of muscle proteins, also raising ethical issues.[29] Moreover, the purity and immunogenicity of the native protein vary greatly within batches. This could affect the reproducibility of CIM.[30] The production of recombinant C-proteins enables a higher throughput although remains more expensive and less affordable (several trials could be required due to poor growth of the organisms of choice for the production, inclusion body formation and protein inactivity[31]). Reproducibility is also affected by several technical aspects, including difficulty in optimising expression and purification and immunogenicity of tags.[32] On the other hand, peptide production is stable, costless (100 USD per gram), has a high throughput and is independent of specific laboratory skills and facilities, hence more reliable. Thus, to overcome these barriers, several groups have attempted to generate IM models using several C-protein polypeptides for immunisation, although without fully reproducing CIM.[21 30]

In light of the above, the present study aimed at optimising the generation and characterisation of the CIM model, taking advantage of an in silico analysis to identify the top three immunogenic and specific regions of C-protein. Mice immunised with the 965–991 aa polypeptide yielded the most severe phenotype (experimental myositis (EM) mice). Cellular and molecular analyses of the muscle further demonstrated similarities with IM. We thus propose EM as an optimised version of CIM.

METHODS

Mice
Eight- to 10-week-old C57BL/6N mice were housed in a temperature- and light-controlled animal facility with food and water ad libitum (Safe Diets, D04, France). Breeding and maintenance were performed according to institutional guidelines. All animal experimental protocols were conducted in an accredited animal house in compliance with French and EU regulations on the use of laboratory animals for research and approved by the Institut de Génétique et de Biologie Moléculaire et Cellulaire Ethical Committee and the French Ministry (#19 395–2019022209557705). Blood was collected by inferior palpebral vein puncture; animals were sacrificed by cervical dislocation, and tissues were collected and immediately processed for biochemical and histological analysis or frozen in liquid nitrogen.

In silico peptide prediction
The top three polypeptides of the human fast-type MYPC were selected by online NHLBI-*AbDesigner*,[33] as the polypeptides with the highest composite score defined by Immunogenicity Score (the highest Ig score), Uniqueness Score (the lowest homology with other MYPC isoforms or other proteins) and Conservation Score (the lowest conservation between mouse and human isoforms) (online supplemental figure 1).

Peptide synthesis
Predicted polypeptides were chemically synthesised in-house on an ABI 433A peptide synthesiser using Fmoc chemistry and purified by reverse phase high-performance liquid chromatography using a preparative scale column (Phenomenex: Kinetex EVO C18, 100 A, 5 µM, 250×21.2 mm).

Immunisation
200 µg of polypeptide in 100 µL phosphate-buffered saline (PBS) were emulsified with an equal volume of complete Freund's adjuvant (FA) (F5881-10 ML, Sigma-Aldrich) and subcutaneously injected on bilateral sides of the hind legs and flanks. Mice injected with the same volume of a saline solution with and without FA were used as controls (ctrl FA and ctrl PBS, respectively). In addition, 2 µg of pertussis toxin (P2980, Sigma-Aldrich) dissolved in 100 µl of PBS were intraperitoneally injected.

Grip test
Forelimb and hindlimb grip strength was determined by Grip Strength Meter (Bioseb) before the immunisation at day (D) 0, at D14 and the day before the sacrifice (D20 or D31). The mean value of three consecutive measurements during the same session was registered as previously described.[34]

Footprint test
The hind feet of the mice were coated with black nontoxic paint.[35] Animals were then allowed to walk along a 50-cm-long, 10-cm-wide runway (with 10-cm-high walls) into an

enclosed box, as described,[35] before the immunisation at D0, at D14 and the day before the sacrifice (D20). All mice had three training runs. A fresh sheet of white paper was placed on the floor of the runway for each run. Hind-base width was measured as the average distance between left and right hind footprints. These values were determined by measuring the perpendicular distance of a given step to a line connecting its opposite preceding and proceeding steps as previously described.[35]

Histochemistry
Muscle specimens (gastrocnemius-soleus, quadriceps, tibialis anterior) collected at sacrifice were rapidly frozen in isopentane cooled in liquid nitrogen and maintained at −80°C until use. Serial 10 µm transverse muscle sections were obtained with a cryostat (LEICA CM3050S) for histochemical staining. Sections were stained with haematoxylin-eosin (H&E) and nicotinamide-adenine dinucleotide (NADH) tetrazolium reductase, as described.[34] Necrosis was defined by pale and/or hyalinised staining on H&E.[36] Regenerating fibres were identified by increased basophilia on H&E-stained sections and/or centronucleated fibres.

Immunostaining
Frozen sections (7 µm) of gastrocnemius muscles collected at sacrifice were fixed in 4% PFA for 15 min at room temperature and permeabilised by 0.5% Triton-X100 for 20 min. Then, blocking of non-specific binding by placing the slides in a dilute solution of 5% non-fat milk powder in TBST (0.1% Tween) for 1 hour was performed. Primary antibody (CD45 Abcam ab10558, dilution 1:200; laminin a-2 Chain Sigma-Aldrich, dilution 1:500; MHC-I Monoclonal Antibody ER-HR52, Santa Cruz Biotechnology, dilution 1:10) was diluted in TBST supplemented with 5% bovine serum albumin and incubated at room temperature for 1 hour. Secondary antibodies conjugated with Alexa Fluor 568 (ab175476; dilution 1:400), Alexa Fluor 488 (112-546-072 Invitrogen; dilution 1:400) or Alexa Fluor 555 (Invitrogen A-21428, dilution 1:400) were diluted in PBS 1X and incubated at room temperature for 45 min. Nuclei were counterstained with DAPI (1:5K; Invitrogen, Eugene, OR, USA). Negative controls were prepared by omitting the primary antibodies and putting only the secondary one or by putting anti-IgG anti-mouse as primary antibodies, later on the secondary antibody.

Microscopic acquisition
Images were acquired using an upright motorised microscope (Leica DM 4000 B) fitted with the CoolSNAP HQ2 (Photometrics) and the Micro-Manager software. Fiji software was used for image editing.[34]

Histological inflammation grading
Inflammation in histological muscle sections was graded as described.[37 38] Briefly, grade 1 was assigned for involvement of <5 muscle fibres; grade 2 for a lesion involving 5–30 muscle fibres; grade 3 for a lesion involving a muscle fasciculus; and grade 4 for diffuse and extensive lesions. Three sections from each block were assessed, and the lesion with the highest grade was selected to calculate the average score. When multiple lesions with the same grade were found in a single sample, 0.5 points were added to the grade.

Necrotic fibres quantification
Quantification of necrotic fibres at D21 was performed as described.[39] Briefly, H&E-stained slides were scanned using the NanoZoomer digital slide scanner (Hamamatsu) and analysed using the NDP.view2 Viewing software (Hamamatsu). The number of necrotic fibres in three muscle sections per animal was determined and averaged.

Cross-sectional area (CSA) and fibre diameter assessment
Tetramethylrhodamine (TRITC)-conjugated wheat germ agglutinin was used for membrane staining (W32464, Thermo Fisher)[40] at 1/500 dilution after paraformaldehyde (PFA) fixation (4%), Triton-X100 0.5% permeabilisation and blocking of non-specific binding by incubation in 5% non-fat dry milk solution.[41] Slides were scanned in fluorescence mode and analysed as described above. Myofibre size, cross-sectional area (CSA) and fibre diameter were determined at D21. The minimum Feret diameter (minFeret) was assessed since the latter is the least affected by distortion due to oblique cross-sectioning of muscle tissue.[42] Muscle fibres were segmented using Cellpose,[43] an artificial intelligence-based programme. The pre-trained 'cyto' model was selected with a diameter set to 50 pixels and the regions of interest (ROI) generated by Cellpose were saved in a Fiji[44] compatible format. Thereafter, the ROI manager of Fiji was used to perform the minimum Feret radius and surface area measurements.

Electron microscopy
Ultrastructural analyses were performed as previously described.[34] Skeletal muscle samples collected at D21 were fixed by immersion in 2.5% glutaraldehyde and 2.5% PFA in cacodylate buffer (0.1 M, pH 7.4), washed in cacodylate buffer for 30 min and stored at 4°C. Postfixation was performed with 1% osmium tetraoxide in 0.1 M cacodylate buffer for 1 hour at 4°C and dehydration through graded alcohol (50, 70, 90 and 100%) and propylene oxide for 30 min each. Samples were oriented longitudinally and embedded in Epon 812. Ultrathin sections were prepared at 70 nm and contrasted with uranyl acetate and lead citrate and examined at 70 kV with a Morgagni 268D electron microscope. Images were captured digitally by a Mega View III camera (Soft Imaging System).

Blood analysis
Blood collected at sacrifice was maintained overnight at 4°C and centrifuged at 400 g for 10 min at 4°C. Serum was stored at −80°C.

CK activity was determined (Creatine Kinase Activity Assay Kit, (MAPK116-1KT, Sigma-Aldrich) in serum according to the manufacturer's protocol.

Muscle RNA extraction and reverse-transcription quantitative PCR (RT-qPCR) analysis

Total RNA was isolated from gastrocnemius muscle at D21 using TRIzol reagent (Invitrogen) according to the manufacturer's instructions. RNA was quantified by spectrophotometry (Nanodrop, Thermo Fisher). cDNA was synthesised from 2 µg RNA by reverse transcription using random primers and SuperScript IV reverse transcriptase (Invitrogen, Life Technologies), according to the manufacturer's protocol. Quantitative reverse-transcription-PCR analysis was performed with selective primers (online supplemental table 1) using the Light Cycler 480 SYBR Green I Master X2 Kit (Roche), according to the manufacturer's protocol. For each sample, the relative abundance of the transcripts of a given gene was normalised to those of a housekeeping gene (18S).

Flow cytometry

Tissue dissociation

Muscle dissociation into single cells was performed following a previously described protocol[45] with minor modifications. Briefly, muscles (gastrocnemius, soleus, tibialis anterior and quadriceps of both legs) were dissected, mechanically minced and enzymatically dissociated in Ham's F-10 (Hyclone) supplemented with 10% horse serum (Life Technologies), 100 units/ml penicillin and 100 µg/mL streptomycin (Omega Scientific) containing 1 mg/mL collagenase type I (17018029 Thermo Fisher Scientific/Gibco) and 5 U/mL dispase (#07913 STEMCELL Technologies) with mild agitation for 60 min in a water bath at 37°C. Cellular clumps were dissociated into single cells by passing the suspension at least 10 times in 5 and 10 mL serological pipettes, followed by 10 times through a 20-gauge needle and a 70 µm cell strainer.

Immunophenotyping experiments

The repertoire of mononuclear cell subpopulations in muscle was established by flow cytometry at D21. Cell suspensions isolated from muscle were incubated with an antibody mixture (online supplemental table 2) for 40 min on ice. Among DAPI-negative cells (living cells), haematopoietic cells were identified by the CD45 marker. Among CD45+cells, lymphocytes were gated according to side scatter, based on their relative size. Two lymphocyte populations were then subsequently gated: CD3+ (T-lymphocytes) and CD3- lymphocytes. Among CD3+cells, CD4+, CD8+ and double negative (DN) cells (CD3+CD4-CD8-) were identified. From CD45+cells, CD11b+cells were gated to select macrophages (F4/80+cells). Among F4/80+cells, Ly6C+and CD206+ macrophages were selected. Data of individual mice were acquired using a BD LSRFortessa Cell Analyzer and analysed using FlowJo software.

Autoantibody assessment

A 96-well plate was coated overnight at 4°C with 2 µg/mL of C-protein polypeptides in PBS. The plate was washed with PBS with 0.05% Tween (PBST) and blocked with 5 mg/mL fish gelatin-blocking buffer (M319-100ML) in PBS for 1 hour. After a washing step, serum (diluted 1:10 in PBS) or muscle (extracted with RIPA lysis buffer and diluted 1:2 in PBS) samples were added into each well (100 µl) and incubated for 1 hour. After three washes, an alkaline phosphatase-conjugated goat anti-mouse secondary antibody (Jackson ImmunoResearch, cat.# 115–055–044) diluted 1:5000 in PBST was added to each well (100 µl) and incubated for 1 hour. The plate was then washed, and colourimetric substrate PNPP was dispensed to the wells and incubated in the dark for 15 min at room temperature. The absorbance at 405 nm was read using a plate spectrophotometer.

Data analysis

No inclusion/exclusion criteria and no method of randomisation were used in this study. No blinding was used for animal studies. A group of mice from independent cohorts was constituted to obtain a sample size with adequate balance between (i) sufficient statistical power and (ii) compliance with the 'Reduction' principle.[46]

The normality of the distributions was verified with the Shapiro-Wilk test. Continuous variables were summarised as median and IQR or mean+SEM according to their distribution. Statistical comparisons of data between two groups were made by a Student's t-test and those between three and more by one-way analysis of variance followed by a post hoc analysis (Tukey's test). Data were considered to be statistically significant if $p < 0.05$ and are indicated by * or $ in the figures.

Statistical analyses were performed using GraphPad Prism 9. The exact significant p values are provided in figure captions.

RESULTS

Immunisation of mice with Freund's adjuvant alone does not induce clinical, histopathological and molecular changes resembling inflammatory myopathies (IM)

Previous studies aiming at characterising rodent models of myositis based on immunisation have used either FA[23 30 47 48] or PBS[49] as controls. None of these control animals displayed characteristics of myositis. Whereas PBS administration is well tolerated, FA produces local and/or systemic pain,[50] questioning the use of FA-treated mice as controls from an ethical perspective. However, to date, these two controls have never been compared.

To investigate whether FA alone induces muscle changes resembling myositis, 8- to 10-week-old mice were treated with a single subcutaneous injection (on both sides of the hind legs and flanks) of FA in PBS (ctrl FA) or of PBS alone (ctrl PBS).

From D0 to D20, grip strength was similar in ctrl FA and ctrl PBS mice (online supplemental figure 2a). No histological lesion (ie, inflammatory infiltrate, necrosis of muscle fibres) was found in gastrocnemius of ctrl FA and ctrl PBS mice (online supplemental figure 2b). Moreover, the transcript levels of type I IFN-stimulated genes (ie, *IFIT3, ISG15*) and type II IFN-stimulated genes (ie, *PSMB8, GBP2*) were similar in ctrl FA and ctrl PBS mice (online supplemental figure 2c).

Together, these results demonstrate that injection with FA does not induce clinical, histopathological and molecular changes resembling IM. Thus, ctrl PBS mice were used as controls in the subsequent experiments.

Amino acids 663–684, 866–890 and 965–991 are the top three potential immunogenic regions of C-protein in mice

The online NHLBI-AbDesigner software was run to identify specific and immunogenic regions of C-protein, encoded by *MYBPC2*.[33] The top three polypeptides fulfilling the following criteria were selected: (i) the highest antigenicity score (immunogenicity); (ii) the lowest homology with other MYPC isoforms or other proteins (uniqueness); (iii) the lowest conservation between mouse and human isoforms to increase peptide immunogenicity in mice (conservation); and (iv) the absence of aa susceptible to post-translational modifications. Peptide 1 (aa 663–684), peptide 2 (aa 866–890) and peptide 3 (aa 965–991) are presented in figure 1a,b. Peptides 2 and 3 are located within one of the two most immunogenic regions of C-protein (fragment 4) identified by Sugihara *et al*.[23]

Immunisation of mice with the synthetic polypeptide encompassing aa 965–991 of C-protein induces muscle weakness, an increase in creatine kinase (CK) levels and muscle histopathological lesions common to inflammatory myopathies (IM)

The production and purification procedure yielded polypeptides of molecular weights of 2497.90 mg/mol (peptide 1), 2743.17 mg/mmol (peptide 2) and 3369.86 mg/mmol (peptide 3) with a purity of 70.4% (peptide 1), 92.7% (peptide 2) and 93.4% (peptide 3), respectively (online supplemental figure 3).

To compare the ability of these peptides to induce myositis, 8- to 10-week-old mice were immunised with a single subcutaneous injection (on both sides of the hind legs and flanks). Mice administered with FA+peptide 3 exhibited a progressive decrease in grip strength from D14 (−32%, p=0.04) to D20 (−44%, p=0.001) after immunisation, whereas the administration of FA+peptide 1 or of FA+peptide 2 had no effect (figure 1c). Immunisation with peptide 3 led to the highest production and accumulation of selective anti-peptide 3 antibodies in muscle (p=0.0008; vs ctrl mice) (figure 1d).

Analysis of H&E stained cryosections from gastrocnemius muscle of FA+peptide 3-treated mice harvested at D21 revealed mononuclear cell infiltration and necrosis of muscle fibres (figure 1e). By contrast, no histological lesion was found in muscle in FA+peptide 1 and FA+peptide 2 treated mice (online supplemental figure 5). Moreover, immunisation with peptide 1 led to less prominent accumulation of anti-peptide 1 antibodies in muscle (p=0.03, vs ctrl mice), and no anti-peptide 2 antibodies were detected after immunisation with peptide 2 (figure 1d). Thus, immunisation with peptide 3 led to the most severe muscle phenotype (EM).

Further characterisation of EM mice highlighted an increase in hind base width at D14 (+22% vs D0, p=0.03) and D20 (+36% vs D0, p=0.0001) (figure 1f; online supplemental figure 6). Moreover, in the serum of EM mice, CK activity at D21 was twofold higher than that of ctrl mice (p=0.005) (figure 1g), and anti-peptide 3 antibodies were also found (p=0.03 vs. ctrl mice) (figure 1h). Antibodies targeting peptides 1 and 2 were also found in muscle (online supplemental figure 4a) and in serum (online supplemental figure 4b) of peptide-3 immunised mice, but at a lower titre, indicating epitope spreading phenomena.[51] Concurrently with the persistence of lower muscle strength of EM mice up to D31 (−23% vs D0, p=0.0001; −21% vs ctrl mice at D31, p=0.0003) (figure 2a), cryosections of the tibialis anterior, gastrocnemius and quadriceps muscles revealed inflammatory infiltrates, necrotic myofibres and numerous small rounded myofibres at D14, D21 and D31 after immunisation (figure 2b; online supplemental figure 7a). A more detailed analysis of the gastrocnemius muscles at D21 revealed that the mononuclear cell infiltrates scored sixfold higher than in controls (p=0.004) (figure 2c) and were located in the endomysial, perimysial and perivascular regions (figure 2b, online supplemental figure 7b). The number of necrotic fibres in EM mice was 10 times higher than in controls (p=0.01) (figure 2d). Fibres CSA and minFeret diameter were reduced by 36% (p=0.03) and 23% (p=0.03), respectively, and the percentage of atrophic fibres (CSA less than or equal to 1000 μm^2) was 2.4-fold higher (p=0.005) in EM mice than in ctrl mice (figure 2e–h). Sarcolemmal expression of MHC-I was found in EM mice, but not in ctrl mice (figure 2i). NADH staining revealed mitochondrial abnormalities, such as linearisation of sarcoplasmic membranes and motheaten fibres (figure 2j). Electron microscopic analysis of gastrocnemius (figure 2k) and quadriceps (online supplemental figure 8) muscles revealed additional lesions of the myofibres including (i) sarcolemmal invagination, (ii) sarcomeric disruption and Z-line misalignments, (iii) T-tubule dilatations and (iv) mitochondria fragmentation.

Taken together, these results demonstrate that EM mice recapitulate several hallmarks of IM, including muscle weakness, myofibre necrosis, atrophy, inflammatory infiltrate, mitochondrial abnormalities and abnormal expression of MHC-I.
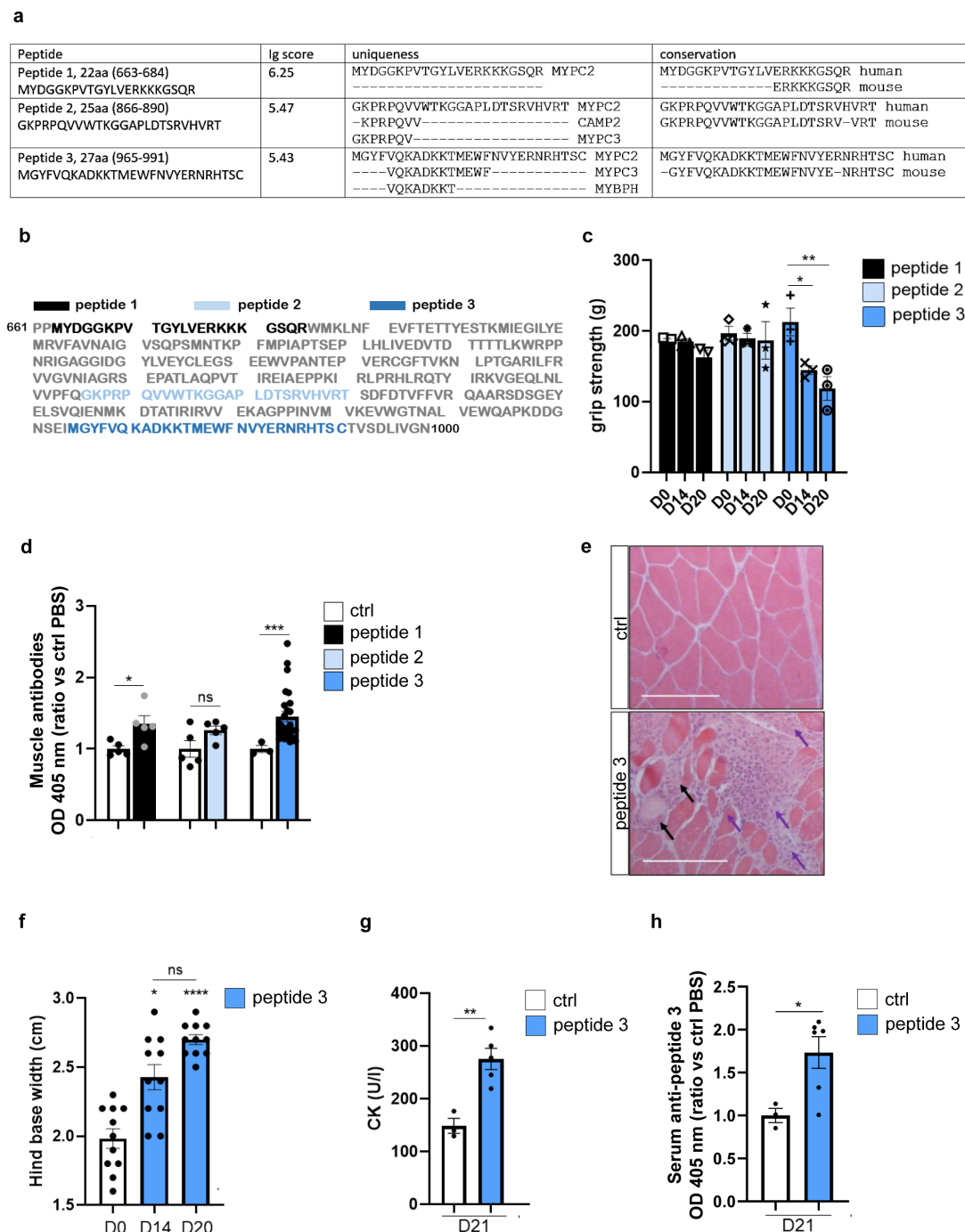
Figure 1 Muscle weakness, walking impairment and muscle lesions in mice treated with polypeptides of human fast-type myosin-binding protein C (MYPC). (a) The predicted features of three polypeptides according to NHLBI-AbDesigner are summarised, in particular Immunogenicity (Ig score), Uniqueness and Conservation Scores. Amino acid sequence of human fast type MYPC. (b) The three polypeptides used for immunisation are identified in coloured text. (c) Grip strength in a cohort of male mice treated with the three C-protein peptides. Muscle strength is expressed as mean±SEM. n=3 per group, two independent cohorts of mice were pooled. *: p=0.04, **: p=0.001 versus day (D) 0. (d) Antibodies targeting the three polypeptides of C-protein (peptides 1, 2 and 3) used for immunisation in gastrocnemius of mice at D21, expressed as the ratio of the absorbance at 405 nm compared with control (ctrl) mice. n≥3 per condition. *p=0.03, ***p=0.0008. ns, not significant. Independent cohorts of male mice were pooled. (e) Representative images of haematoxylin and eosin (H&E) staining of gastrocnemius muscle sections from peptide 3-treated and control male mice at D21. Necrotic fibres (pale fibres) and immune cell infiltrations are indicated by black and purple arrows, respectively. Scale bar: 100 µm. (f) Footprint test performed in female mice treated with peptide 3 at D0, D14 and D20. Hind base width was measured (cm) and expressed as mean±SEM (n=11, three independent cohorts of mice). *p=0.03, ****p<0.0001. (g) Serum creatine kinase levels at D21 in female mice immunised with peptide 3 compared with ctrl. n≥3 per condition. Two independent cohorts of mice were pooled. **p=0.005. (h) Serum anti-peptide 3 antibodies at D21 expressed as ratio of the absorbance at 405 nm compared with ctrl mice. n ≥3 per condition. Two independent cohorts of female mice were pooled. *p=0.03.
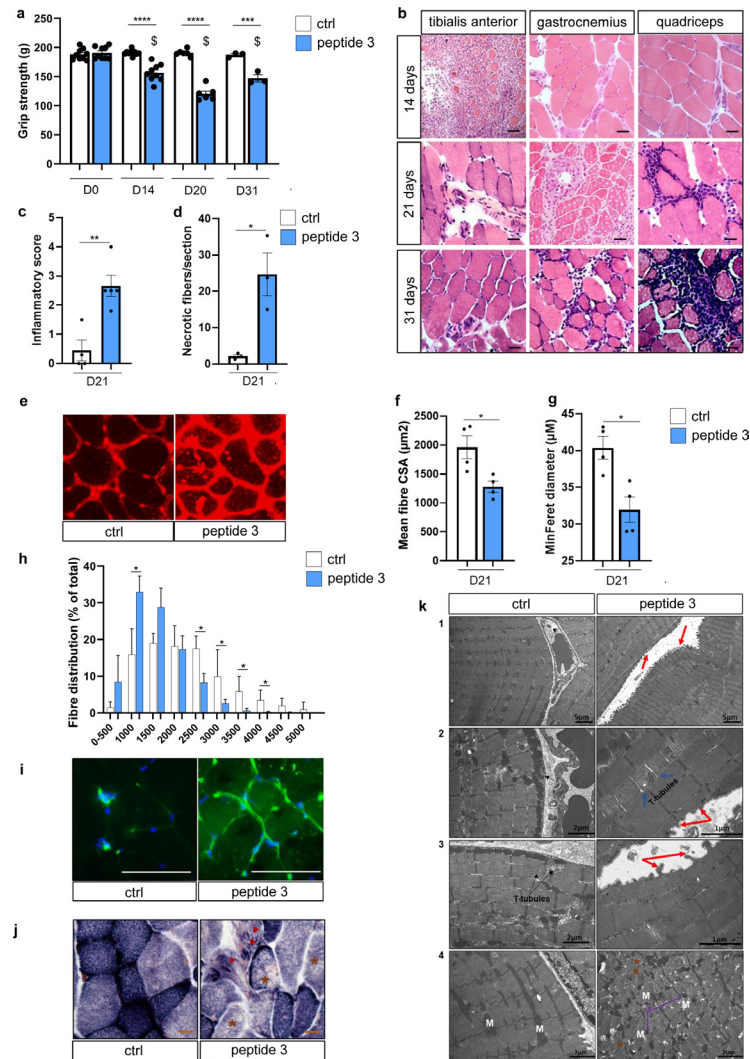
Figure 2 Characterisation of muscle impairment in female mice treated with a peptide encompassing amino acids 965–991 (peptide 3) of fast-type skeletal muscle C-protein. (a) Grip strength measurements in mice at day 0 (D0), 14 (D14), 20 (D20) and 31 (D31) after subcutaneous (SC) administration of the peptide 3. Mice injected with phosphate-buffered saline (PBS) were used as controls. Muscle strength is expressed as mean±SEM. n ≥ 3 per group. Two independent cohorts of mice were pooled. ****$p < 0.0001$, ***$p = 0.0003$ compared with control (ctrl) at the same timepoint; \$$p < 0.0001$ versus grip strength at D0 in peptide 3-treated mice. (b) Representative images of haematoxylin and eosin (H&E) staining of tibialis anterior, gastrocnemius and quadriceps cryosections at D14, D21 and D31 after immunisation with peptide 3. n ≥3 per condition. Two independent cohorts of mice were pooled. Scale bar: 50 µm. (c) Histological inflammatory infiltrate score in H&E-stained slides from control and peptide 3-treated mice at D21. Each dot represents the average score of three sections for each mouse (n=4 for each condition from more than two independent cohorts of mice). (d) Necrotic fibre quantification in H&E-stained sections from control and peptide 3-treated mice at D21. The number of necrotic fibres in three muscle sections per mouse (n=3 for each condition from two independent cohorts of mice) was determined and averaged. (e) Wheat germ agglutinin TRITC-conjugated staining in gastrocnemius cryosections from control and peptide 3-treated mice at D21. Slides were scanned in fluorescence mode and analysed to determine fibre size. Cross-sectional area (CSA) (f) and minimum Feret diameter (minFeret) (g) measurements on gastrocnemius cryosections from control and peptide 3-treated mice at D21. *: $p = 0.03$. Results are expressed as mean±SEM. Each dot represents the average results for one mouse (n=4 from two independent cohorts of mice). (h) Size distribution of 16 040 and 20 111 fibres from the gastrocnemius muscle of mice treated with peptide 3 (n=4 from two independent cohorts of mice) and ctrl mice (n=4 from two independent cohorts of mice), respectively, at D21. *$p < 0.05$. (i) Representative images of major histocompatibility complex-I staining (green) in gastrocnemius muscle from control and peptide 3-treated mice (n=3 for each condition from two independent cohorts of mice) at D21. Nuclei were counterstained with 4′,6-diamidino-2-phenylindole (DAPI, blue). Scale bar: 50 µm. (j) Representative images of mitochondrial abnormalities assessed by reduced nicotinamide adenine dinucleotide (NADH) tetrazolium reductase staining in gastrocnemius muscle at D21. Motheaten fibres (brown asterisk) and linearisation of sarcoplasmic membranes (red arrowheads) are shown (n=3 for each condition from two independent cohorts of mice). (k) Representative images of electron microscopy analysis of gastrocnemius muscle at D21 in control and peptide 3-treated mice (n=3 for each condition from two independent cohorts of mice). Sarcomeric disruption (panel 4), Z-line misalignments (brown asterisk), T-tubule dilatations (light blue arrows), sarcolemmal invagination (red arrows) and mitochondrial (white M) fragmentation (violet arrows) are shown in peptide 3-treated mice.

Muscle from experimental myositis mice displays a pro-inflammatory environment resembling inflammatory myopathies (IM)

To further assess the similarities between EM and IM at the cellular and molecular levels, a comprehensive analysis of the immune compartment and IFN-stimulated transcripts were performed in muscle of EM mice at D21.

Flow cytometry analysis (online supplemental figure 9) revealed that the proportion of CD45+ cells (immune cells) was 12-fold higher in EM mice than in ctrl mice (16.8 (10.5–19.4) vs 1.4% (0.8–5) of singlets, p=0.04) (figure 3a).

The CD11b+/CD45+ cells ratio (myeloid cells/immune cells) and the F4/80+/CD11b+ cells (macrophages/myeloid cells) were similar in EM and ctrl mice (figure 3b). Nevertheless, the Ly6c+/F4/80+ cell ratios (pro-inflammatory/total macrophages) was 1.7-fold higher (76.1 (56.6–81.8) vs 45.1% (44.1–47.3), p=0.01) while that of CD206+/F4/80+cells (anti-inflammatory/total macrophages) was 1.7-fold lower (16.8 (14.5–16.9) vs 29% (26.2–31.2), p=0.007) in EM mice (figure 3c). The CD3+/lymphocyte ratio (T lymphocytes/total lymphocytes according to side scatter) and the CD3-/lymphocytes ratio (non-T lymphocytes/total lymphocytes according to side scatter) were similar in EM mice and ctrl mice (42.9 (30.7–53.1) vs 34.3% (31.2–53.3), p=0.7; 52.4 (44.3–59.3) vs 45.9% (41.2–60.2), p=0.7, respectively) (figure 3d). However, the CD8+/CD3+ cell ratio (31.5 (22.1–34.7) vs 1.3% (0.6–5.4), p=0.001) and the CD4+/CD3+cells ratio (39.7 (26.8–59) vs 4.5% (2.6–10.5), p=0.007) were higher in EM mice. Conversely, the CD4-CD8-/CD3+ cells ratio (82.3 (78.8–94.9) vs 26.2% (12.9–35), p<0.0001) (figure 3e), as well as CD25+/CD4+ cells ratio (24.9 (22–26.3) vs 6.2% (4.1–6.8), p=0.0002) (figure 3f), were higher in ctrl mice, indicating the prevalence of T-lymphocytes with a pro-inflammatory phenotype in EM mice.

Moreover, the transcript levels of several type I IFN-stimulated genes (ie, *IFIT3, IFI44, RSAD2*) were two- to 10fold higher (figure 3g) in the gastrocnemius muscle of EM mice, while transcript levels of several type II IFN-stimulated genes (*PSMB8, GBP2, GBP1, CXCL9*) were increased by two- to seven-fold (figure 3h).

Together, these results indicate that EM mice show a pro-inflammatory muscle environment that resembles IM regardless of disease subtype.

DISCUSSION

Previous attempts to overcome the technical limits of CIM using C-protein polypeptides have failed to reproduce the characteristics of IM in mice.[21] Such polypeptides are located within the most immunogenic region according to Sugihara *et al* (fragment 2, aa 284–580).[23]

Based on in silico immunogenicity prediction, we identified a polypeptide encompassing aa 965–991 of C-protein, which was synthesised with a high purity. Both in male and female mice, this polypeptide induced muscle weakness after a single immunisation. In addition, we show in female mice that this polypeptide induced a reproducible experimental IM model (EM) in several independent cohorts of mice, recapitulating the hallmarks common to all IM subtypes at the clinical, histological, cellular and molecular levels, including autoantibodies that have been recently discovered as main actors in the IM pathogenesis.[17] In compliance with the 'Reduction' principle,[46] the sample sizes of the groups were minimised. As a consequence, the statistical power is limited for some parameters (eg, cellular and molecular characteristics) which might be further refined in the future.

EM has several advantages compared with CIM. Polypeptide production is low cost and does not require specific laboratory facilities. This makes polypeptide production more affordable and reliable and enables harmonisation of the results. Similarly to CIM, the C57BL/6N background facilitates the potential induction of EM in genetically engineered mice which could prove valuable in fostering preclinical research in IM.

Using solely a polypeptide portion of the C-protein, we were able to confirm previous findings obtained in CIM mice including decreased exercise capacity, endomysial, perimysial and perivascular mononuclear cell infiltrates (T cells and macrophages) within the muscle as well as serum antibodies targeting C-protein.[23]

We additionally provide new insights in the characterisation of the model by demonstrating muscle weakness, increased serum CK levels, muscle fibre lesions (ie, MHC-I expression, atrophy, mitochondrial abnormalities, sarcolemmal irregularities, sarcomeric disruptions and necrosis), immune cell compartment imbalance, type 1 and 2 IFN-signature, and antibodies targeting the polypeptide of C-protein used for immunisation within the muscle.

Data indicate a role of autoantibodies in IM pathogenesis.[17] We found that the amounts of anti-C protein antibodies obtained after peptides 1, 2 and 3 immunisation were positively associated with the phenotypic severity. This suggests antibodies might play a pathogenic role in EM mice.

Using histology, immunostaining and flow cytometry, CD4+ and CD8+ T cells were found in the muscles from peptide 3-treated mice. Adoptive transfer experiments were not performed in EM to further investigate the role of CD4+ and CD8+ cells. However, previous reports show that (i) the T-cell population of EM was similar to that found in both muscle and lymph nodes of mice immunised with partially purified myosin;[47] (ii) the transfer of antigen-sensitised or CD4+-sorted cells from the lymph nodes of these mice has been shown to induce myositis in naïve, irradiated, recipient mice;[47] and (iii) CD8+ T-cells play a critical role in mediating muscle injury in CIM[28] as well as in human disease.[52] Interestingly, we found low levels of DN (CD3+CD4-CD8-) T-cells in EM. DN T-cells are characterised by the capability of inhibiting an immune response via directly killing effector T cells in an antigen-specific fashion, partially mediated by
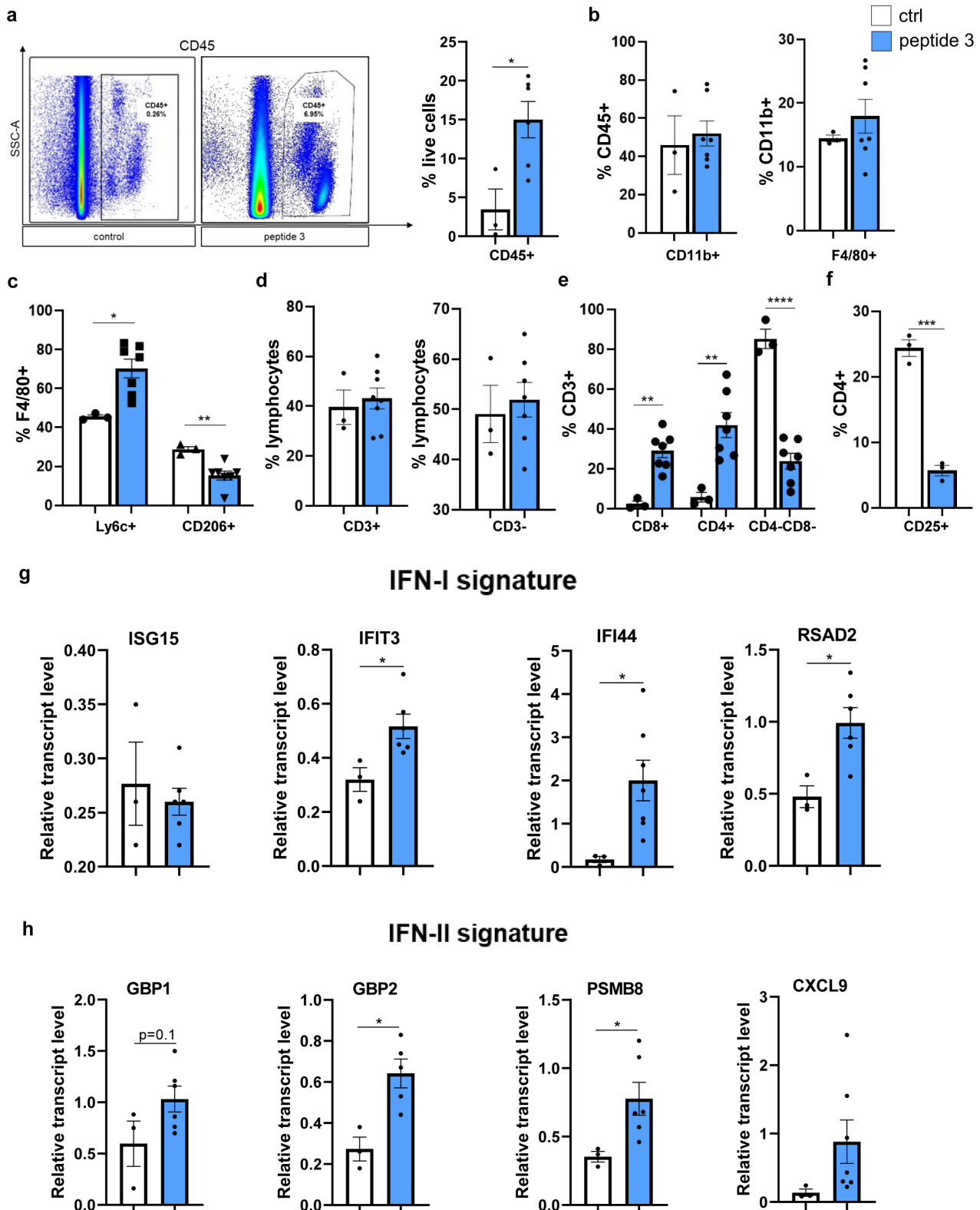
Figure 3 Characterisation of the muscle pro-inflammatory environment in female mice treated with a peptide encompassing amino acids 965–991 (peptide 3) of human fast-type myosin-binding-protein C (MYPC). Flow cytometry analysis performed on muscle (anterior tibialis, gastrocnemius, quadriceps) from peptide 3-treated mice (n ≥3) and control mice (n ≥3) from independent cohorts: (a) representative image of the gating strategy used to select CD45+ cells (immune cells) and lymphocytes. *p=0.02. (b) Myeloid compartment. (c) Macrophage distribution. *p=0.01; **p=0.007. (d) Lymphocyte distribution. (e) T-lymphocyte distribution (CD3+cells). **p<0.01; ****p<0.0001. (f) Regulatory T-cells (CD4+ CD25+ cells). ***p=0.0002. Each bar represents the mean±SEM. (g, h) Relative transcript levels of (g) interferon (IFN) I and (h) IFN-II signature in gastrocnemius muscle of control and peptide 3-treated mice (n ≥3 for each condition from independent cohorts of mice). The levels were normalised to the 18S gene (housekeeping). *p<0.05.

the acquisition of MHC-peptide complexes from antigen presenting cells.[53] Thus, in EM, low levels of the DN T-cell population might contribute to the pro-inflammatory phenotype of the immune cell infiltrate.

Muscle inflammation in CIM was previously shown to begin resolving after D28 while muscle function was not assessed at this time point.[23] Of note, in the present study, clinical and biological phenotypes in EM persisted for at least 31 days, thus providing a larger experimental window.

Although the exact pathophysiological mechanisms of IM are unknown, data indicate that some mechanisms are shared by all IM subtypes,[6] whereas others are subtype-specific.[13] This observation probably explains that certain current therapeutic strategies improve all IM subtypes (ie, corticosteroids, rituximab), while others are only effective in some subgroups.[54] EM may represent an advantage in a strategy aimed at deciphering the underlying mechanisms and/or testing the efficacy of targeting common mechanisms of IM. However, this may also represent a limitation in a strategy aiming at deciphering subtype-specific aspects of the disease. For example, the specific role of autoantigens and/or autoantibodies is unlikely to be answered by EM, but possibly addressed by other animal models (eg, based on immunisation against specific autoantigens[48] or on the transfer of specific autoantibodies).

EM mice are an optimised and characterised version of CIM that recapitulates common hallmarks of IM. This costless, high-throughput, reliable and stable model, obtained in the most commonly used background for genetic engineering in mice (C57BL/6N), may foster a better understanding and preclinical treatment of IM.

Author affiliations
[1]Physiology and Muscle function explorations, University hospital of Strasbourg, Strasbourg, France
[2]UR3072 "mitochondrie, stress oxydant et plasticité musculaire", Centre de recherche en biomédecine, Strasbourg, France
[3]University of Strasbourg, CNRS UMR7104, INSERM U1258, IGBMC, Illkirch, France
[4]Inserm UMS 38, Centre de Recherche en Biomédecine de Strasbourg, PIC-STRA, Faculté de Médecine, University of Strasbourg, Strasbourg, France
[5]Physiology and function explorations, University hospital of Strasbourg, Strasbourg, France
[6]Rheumatology Department, Centre de Référence des Maladies Autoimmunes Rares, Strasbourg, France

X Margherita Giannini @giannini85

ORCID iDs
Margherita Giannini http://orcid.org/0000-0002-4834-5804
Alain Meyer http://orcid.org/0000-0003-0893-6041

REFERENCES

1. Debrut L, Giannini M, Klein D, et al. Refining Incidence and Characteristics of Inflammatory Myopathies: A Quadruple-Source Capture-Recapture Survey Using the 2017 European League Against Rheumatism/American College of Rheumatology Classification Criteria. *Arthritis Rheumatol* 2023;75:1850–5.
2. Meyer A, Lannes B, Goetz J, et al. Inflammatory myopathies: A new landscape. *Joint Bone Spine* 2018;85:23–33.
3. Mariampillai K, Granger B, Amelin D, et al. Development of a New Classification System for Idiopathic Inflammatory Myopathies Based on Clinical Manifestations and Myositis-Specific Autoantibodies. *JAMA Neurol* 2018;75:1528–37.
4. Giannini M, Ellezam B, Leclair V, et al. Scleromyositis: A distinct novel entity within the systemic sclerosis and autoimmune myositis spectrum. Implications for care and pathogenesis. *Front Immunol* 2022;13:974078.
5. Lundberg IE, Tjärnlund A, Bottai M, et al. 2017 European League Against Rheumatism/American College of Rheumatology classification criteria for adult and juvenile idiopathic inflammatory myopathies and their major subgroups. *Ann Rheum Dis* 2017;76:1955–64.
6. Amici DR, Pinal-Fernandez I, Christopher-Stine L, et al. A network of core and subtype-specific gene expression programs in myositis. *Acta Neuropathol* 2021;142:887–98.
7. Hoogendijk JE, Amato AA, Lecky BR, et al. 119th ENMC international workshop: Trial design in adult idiopathic inflammatory myopathies, with the exception of inclusion body myositis, 10–12 October 2003, Naarden, The Netherlands. *Neuromuscul Disord* 2004;14:337–45.
8. Meyer A, Laverny G, Allenbach Y, et al. IFN-β-induced reactive oxygen species and mitochondrial damage contribute to muscle impairment and inflammation maintenance in dermatomyositis. *Acta Neuropathol* 2017;134:655–66.
9. Aguilar-Vazquez A, Chavarria-Avila E, Salazar-Paramo M, et al. Impaired muscle strength is associated with ultrastructure damage in myositis. *Sci Rep* 2022;12:17671.

10 Zhang D, Zhang DE. Interferon-stimulated gene 15 and the protein ISGylation system. *J Interferon Cytokine Res* 2011;31:119–30.

11 D'Cunha J, Ramanujam S, Wagner RJ, *et al*. In vitro and in vivo secretion of human ISG15, an IFN-induced immunomodulatory cytokine. *J Immunol* 1996;157:4100–8.

12 Hall JC, Baer AN, Shah AA, *et al*. Molecular Subsetting of Interferon Pathways in Sjögren's Syndrome. *Arthritis Rheumatol* 2015;67:2437–46.

13 Pinal-Fernandez I, Casal-Dominguez M, Derfoul A, *et al*. Machine learning algorithms reveal unique gene expression profiles in muscle biopsies from patients with different types of myositis. *Ann Rheum Dis* 2020;79:1234–42.

14 Hisamatsu H, Shimbara N, Saito Y, *et al*. Newly identified pair of proteasomal subunits regulated reciprocally by interferon gamma. *J Exp Med* 1996;183:1807–16.

15 Hall JC, Casciola-Rosen L, Berger AE, *et al*. Precise probes of type II interferon activity define the origin of interferon signatures in target tissues in rheumatic diseases. *Proc Natl Acad Sci U S A* 2012;109:17609–14.

16 Vattemi G, Mirabella M, Guglielmi V, *et al*. Muscle biopsy features of idiopathic inflammatory myopathies and differential diagnosis. *Auto Immun Highlights* 2014;5:77–85.

17 Pinal-Fernandez I, Muñoz-Braceras S, Casal-Dominguez M, *et al*. Pathological autoantibody internalisation in myositis. *Ann Rheum Dis* 2024;83:1549–60.

18 Leclair V, Regardt M, Wojcik S, *et al*. Health-Related Quality of Life (HRQoL) in Idiopathic Inflammatory Myopathy: A Systematic Review. *PLoS One* 2016;11:e0160753.

19 Dobloug GC, Svensson J, Lundberg IE, *et al*. Mortality in idiopathic inflammatory myopathy: results from a Swedish nationwide population-based cohort study. *Ann Rheum Dis* 2018;77:40–7.

20 Meyer A, Scirè CA, Talarico R, *et al*. Idiopathic inflammatory myopathies: state of the art on clinical practice guidelines [corrected]. *RMD Open* 2018;4:e000784.

21 Afzali AM, Ruck T, Wiendl H, *et al*. Animal models in idiopathic inflammatory myopathies: How to overcome a translational roadblock? *Autoimmun Rev* 2017;16:478–94.

22 Okiyama N, Sugihara T, Iwakura Y, *et al*. Therapeutic effects of interleukin-6 blockade in a murine model of polymyositis that does not require interleukin-17A. *Arthritis Rheum* 2009;60:2505–12.

23 Sugihara T, Sekine C, Nakae T, *et al*. A new murine model to define the critical pathologic and therapeutic mediators of polymyositis. *Arthritis Rheum* 2007;56:1304–14.

24 Sugihara T, Okiyama N, Watanabe N, *et al*. Interleukin-1 and tumor necrosis factor α blockade treatment of experimental polymyositis in mice. *Arthritis Rheum* 2012;64:2655–62.

25 Kamiya M, Mizoguchi F, Kawahata K, *et al*. Targeting necroptosis in muscle fibers ameliorates inflammatory myopathies. *Nat Commun* 2022;13:166.

26 Umezawa N, Kawahata K, Mizoguchi F, *et al*. Interleukin-23 as a therapeutic target for inflammatory myopathy. *Sci Rep* 2018;8:5498.

27 Okiyama N, Hasegawa H, Oida T, *et al*. Experimental myositis inducible with transfer of dendritic cells presenting a skeletal muscle C protein-derived CD8 epitope peptide. *Int Immunol* 2015;27:327–32.

28 Sugihara T, Okiyama N, Suzuki M, *et al*. Definitive engagement of cytotoxic CD8 T cells in C protein-induced myositis, a murine model of polymyositis. *Arthritis Rheum* 2010;62:3088–92.

29 Offer G, Moos C, Starr R. A new protein of the thick filaments of vertebrate skeletal myofibrils. *J Mol Biol* 1973;74:653–76.

30 Matsumoto Y, Kohyama K, Park IK, *et al*. Characterization of pathogenic T cells and autoantibodies in C-protein-induced autoimmune polymyositis. *J Neuroimmunol* 2007;190:90–100.

31 Rosano GL, Ceccarelli EA. Recombinant protein expression in Escherichia coli: advances and challenges. *Front Microbiol* 2014;5:172.

32 Jia B, Jeon CO. High-throughput recombinant protein expression in Escherichia coli: current status and future perspectives. *Open Biol* 2016;6:160196.

33 Pisitkun T, Hoffert JD, Saeed F, *et al*. NHLBI-AbDesigner: an online tool for design of peptide-directed antibodies. *Am J Physiol Cell Physiol* 2012;302:C154–64.

34 Gali Ramamoorthy T, Laverny G, Schlagowski A-I, *et al*. The transcriptional coregulator PGC-1β controls mitochondrial function and anti-oxidant defence in skeletal muscles. *Nat Commun* 2015;6:10210.

35 Carter RJ, Lione LA, Humby T, *et al*. Characterization of progressive motor deficits in mice transgenic for the human Huntington's disease mutation. *J Neurosci* 1999;19:3248–57.

36 Available: https://neuromuscular.wustl.edu/pathol/necrosis.htm

37 Kojima T, Tanuma N, Aikawa Y, *et al*. Myosin-induced autoimmune polymyositis in the rat. *J Neurol Sci* 1997;151:141–8.

38 Kohyama K, Matsumoto Y. C-protein in the skeletal muscle induces severe autoimmune polymyositis in Lewis rats. *J Neuroimmunol* 1999;98:130–5.

39 Arnold L, Perrin H, de Chanville CB, *et al*. CX3CR1 deficiency promotes muscle repair and regeneration by enhancing macrophage ApoE production. *Nat Commun* 2015;6:8972.

40 Lim HW, De Windt LJ, Steinberg L, *et al*. Calcineurin expression, activation, and function in cardiac pressure-overload hypertrophy. *Circulation* 2000;101:2431–7.

41 Lionello VM, Nicot A-S, Sartori M, *et al*. Amphiphysin 2 modulation rescues myotubular myopathy and prevents focal adhesion defects in mice. *Sci Transl Med* 2019;11:eaav1866.

42 Briguet A, Courdier-Fruh I, Foster M, *et al*. Histological parameters for the quantitative assessment of muscular dystrophy in the mdx-mouse. *Neuromuscul Disord* 2004;14:675–82.

43 Stringer C, Wang T, Michaelos M, *et al*. Cellpose: a generalist algorithm for cellular segmentation. *Nat Methods* 2021;18:100–6.

44 Schindelin J, Arganda-Carreras I, Frise E, *et al*. Fiji: an open-source platform for biological-image analysis. *Nat Methods* 2012;9:676–82.

45 Liu L, Cheung TH, Charville GW, *et al*. Isolation of skeletal muscle stem cells by fluorescence-activated cell sorting. *Nat Protoc* 2015;10:1612–24.

46 Available: https://caat.jhsph.edu/the-principles-of-humane-experimental-technique

47 Allenbach Y, Solly S, Grégoire S, *et al*. Role of regulatory T cells in a new mouse model of experimental autoimmune myositis. *Am J Pathol* 2009;174:989–98.

48 Okiyama N, Ichimura Y, Shobo M, *et al*. Immune response to dermatomyositis-specific autoantigen, transcriptional intermediary factor 1γ can result in experimental myositis. *Ann Rheum Dis* 2021;80:1201–8.

49 Schneider C, Matsumoto Y, Kohyama K, *et al*. Experimental autoimmune myositis in the lewis rat: lack of spontaneous T-cell apoptosis and therapeutic response to glucocorticosteroid application. *J Neuroimmunol* 2000;107:83–7.

50 Available: https://oacu.oir.nih.gov/system/files/media/file/2022-04/b8_adjuvants.pdf

51 Vanderlugt CL, Miller SD. Epitope spreading in immune-mediated diseases: implications for immunotherapy. *Nat Rev Immunol* 2002;2:85–95.

52 Hofbauer M, Wiesener S, Babbe H, *et al*. Clonal tracking of autoaggressive T cells in polymyositis by combining laser microdissection, single-cell PCR, and CDR3-spectratype analysis. *Proc Natl Acad Sci U S A* 2003;100:4090–5.

53 Chen W, Ford MS, Young KJ, *et al*. The role and mechanisms of double negative regulatory T cells in the suppression of immune responses. *Cell Mol Immunol* 2004;1:328–35.

54 Tjärnlund A, Tang Q, Wick C, *et al*. Abatacept in the treatment of adult dermatomyositis and polymyositis: a randomised, phase IIb treatment delayed-start trial. *Ann Rheum Dis* 2018;77:55–62.